IASLC

ORIGINAL ARTICLE

Preclinical Modeling of Osimertinib for NSCLC With *EGFR* Exon 20 Insertion Mutations

Yusoo Lee,[a] Tae Min Kim, MD, PhD,[a,b,*] Dong-Wan Kim, MD, PhD,[a,b]
Soyeon Kim, PhD,[a,c] Miso Kim, MD,[a,b] Bhumsuk Keam, MD, PhD,[a,b] Ja-Lok Ku, PhD,[a]
Dae Seog Heo, MD, PhD[a,b]

[a]*Seoul National University Cancer Research Institute, Seoul, Republic of Korea*
[b]*Department of Internal Medicine, Seoul National University Hospital, Seoul, Republic of Korea*
[c]*Biomedical Research Institute, Seoul National University Hospital, Seoul, Republic of Korea*

ABSTRACT

Introduction: NSCLC with *EGFR* exon 20 insertion mutations is the third most common type of *EGFR*-mutant NSCLC and is resistant to EGFR tyrosine kinase inhibitors (TKIs). This study was conducted to evaluate the efficacies of first- to third-generation EGFR TKIs against NSCLC cells harboring *EGFR* exon 20 insertion mutations.

Methods: We developed seven *EGFR* exon 20 insertionmutant Ba/F3 models and one patient-derived NSCLC (SNU-3173) of subtypes A763insFQEA, V769insASV, D770insSVD, D770insNPG, P772insPR, H773insH, H773insNPH, and H773insAH. Cell viability assays, immunoblotting, and N-ethyl-N-nitrosourea mutagenesis screenings were performed. *EGFR* exon 20 insertion–mutant structures and couplings with osimertinib, a third-generation EGFR TKI, were modeled and compared.

Results: *EGFR* exon 20 insertion–mutant NSCLC cells, excluding *EGFR* A763insFQEA, were resistant to first-generation EGFR TKIs (concentration that inhibits 50% [IC_{50}], 1.1 ± 0.067 to 5.4 ± 0.115 μM). Mutants were sensitive to second-generation EGFR TKIs (IC_{50}, 0.02 ± 0.0002 to 161.8 ± 18.7nM), except *EGFR* H773insH (IC_{50}, 46.3 ± 8.0 to 352.5 ± 22.7nM). The IC_{50} ratios for mutant to wild-type cells were higher than those for third-generation EGFR TKIs. Third-generation EGFR TKI osimertinib was highly potent against *EGFR* exon 20 insertion–mutant cells (IC_{50}, 14.7-62.7 nM), including *EGFR* H773insH, and spared wild-type EGFR cells. N-ethyl-N-nitrosourea mutagenesis screening of *EGFR* exon 20 insertion–mutant Ba/F3 cells showed various second sites for *EGFR* mutations, mostly at exons 20 and 21, including E762K, P794S, and G796D. In addition, osimertinib-resistant cells were established by stepwise exposure to osimertinib and harbored *EGFR* E762K mutation.

Conclusions: Osimertinib is active against *EGFR* exon 20 insertion–mutant NSCLC and flexibly binds within drug-binding pockets in preclinical models.

© 2019 International Association for the Study of Lung Cancer. Published by Elsevier Inc. All rights reserved.

Keywords: Osimertinib; NSCLC; *EGFR* exon 20 insertion; Resistance

Introduction

Lung cancer is the leading cause of cancer-related deaths worldwide and in Korea.[1,2] Most lung cancers are diagnosed as NSCLC, of which lung adenocarcinoma is the most common subtype in Korea.[1] EGFR-mutant lung adenocarcinoma is a major molecular subtype of NSCLC, representing approximately 60% of lung adenocarcinomas in Korea.[3,4] The most common activating *EGFR* mutations are exon 19 in-frame deletion and

L858R substitution. These mutations account for more than 80% of EGFR-activating mutations and are sensitive to EGFR tyrosine kinase inhibitors (TKIs).[5]

EGFR exon 20 insertion mutations in the αC-β4 loop activate EGFR in a ligand-independent manner and are observed in approximately 4% of *EGFR*-mutant NSCLCs.[6] These mutations cluster between amino acids 767 and 775 of the αC-β4 loop, but rarely occur within the αC-helix (amino acids 761-766) or β4-strand. NSCLCs with *EGFR* exon 20 insertion mutations, except for *EGFR* A763insFQEA, show primary resistance to the reversible EGFR TKIs gefitinib and erlotinib and the irreversible EGFR TKIs neratinib, afatinib, and dacomitinib.[6] Median progression-free survival (PFS) of NSCLC patients with *EGFR* exon 20 insertion mutations who received afatinib was 2.7 months in a combined post hoc analysis of LUX-Lung 2, 3, and 6.[7] Poziotinib showed promising efficacy initially with an objective response rate (ORR) of 64% in NSCLC patients with *EGFR* exon 20 insertion mutations.[8] However, updated results showed median PFS of 5.5 months with dose reduction in 60% of patients with *EGFR* exon 20 mutations.[9]

Despite being the third most common type of *EGFR* mutation, multiple subtypes and structural differences among *EGFR* exon 20 insertion mutations may limit the development of novel targeted therapies. In this study, we developed seven Ba/F3 models of relatively common *EGFR* exon 20 insertion mutations and a patient-derived cell line to evaluate the efficacies of first- to third-generation EGFR TKIs. In addition, in silico homology models of the structures of *EGFR* exon 20 insertion mutations were constructed, and subtypes were compared. Osimertinib, a third-generation EGFR TKI, was highly active against NSCLC with *EGFR* exon 20 insertion mutation without affecting wild-type EGFR. Potential mechanisms of resistance to osimertinib in *EGFR* exon 20 insertion–mutant NSCLC were identified by N-Ethyl-N-nitrosourea (ENU) mutagenesis screening.

Materials and Methods
Cell Lines and Reagents

293T/17 (ATCC CRL-11268), *KRAS*[G12S]-mutant A549 (ATCC CCL-185), and *EGFR*[L858R/T790M]-mutant NCI-H1975 (ATCC CRL-5908) cell lines were purchased from American Type Culture Collection (ATCC; Manassas, Virginia). The *EGFR*[E746-A750del]-mutant PC9 cell line was kindly provided by Mayumi Ono (Kyushu University, Fukuoka, Japan). Ba/F3, a mouse pro-B-cell line, was purchased from Deutsche Sammlung von Mikroorganismen und Zellkulturen (DSMZ; Braunschweig, Germany). SNU-3173 cells were derived at diagnosis from a 46-year-old male patient with stage IV NSCLC with *EGFR* H773insAH mutation who failed after one cycle of

pemetrexed and cisplatin and subsequently died 3 months after diagnosis (Institutional Review Board [IRB] No. 1102-098-357). SNU-3173, PC9, A549, and NCI-H1975 cells were grown in Roswell Park Memorial Institute (RPMI)–1640 media supplemented with 10% fetal bovine sera (FBS; Gibco, Waltham, Massachusetts) and 1% penicillin/streptomycin (Gibco). Ba/F3 cells were grown in RPMI-1640 media supplemented with 10% FBS, 1% penicillin/streptomycin, 2 mmol/L L-glutamine, and 4 ng/mL interleukin (IL)–3 (ProSpec, Rehovot, Israel). 293T/17 cells were grown in Dulbecco's Modified Eagle Medium supplemented with 10% FBS and 2 mmol/L L-glutamine. Erlotinib, gefitinib, afatinib, dacomitinib, nazartinib, olmutinib, osimertinib, and rociletinib were purchased from Selleck Chemicals (Boston, Massachusetts).

Site-Directed Mutagenesis and Construction of Retroviral Vector-Transduced Ba/F3 Cells

EGFR exon 20 insertion variant cDNAs were generated by site-directed mutagenesis (Agilent Technologies, Santa Clara, California) of wild-type *EGFR* in retroviral vector pBABE-puro. The pBABE wild-type EGFR, *EGFR* insertion H (H773insH), and *EGFR* D770_N771insNPG (D770insNPG) were kindly provided by Matthew Meyerson (Dana-Farber Cancer Research Institute, Boston, Massachusetts; Addgene plasmids #11011, #32067, and #11016, respectively) with primers specific for the mutant constructs (Supplementary Table 1).[10] Mutant cDNAs were inserted into TOPO-TA cloning vector (Invitrogen, Carlsbad, California) and analyzed by electropherogram, which was further confirmed with The Basic Local Alignment and Search Tool (BLAST; National Center for Biotechnology Information, Bethesda, Maryland). Each *EGFR* exon 20 insertion variant construct was transfected into Ba/F3 cells. Retroviral-transduced Ba/F3 cells were selected by puromycin treatment and subsequently cultured in IL-3–free media for 4 weeks.

Cell Proliferation Assays

Ba/F3 cells constructed with *EGFR* exon 20 insertion variants were cultured in 96-well plates with RPMI-1640 media containing EGFR TKIs for 72 hours. EGFR TKIs including erlotinib, gefitinib, afatinib, dacomitinib, nazartinib, olmutinib, osimertinib, and rociletinib, were serially diluted 10-fold from 10 μM to 10 pM. Cell proliferation was analyzed using CellTiter Glo-Luminescent cell viability assay (Promega, Madison, Wisconsin). The luminescent signal was measured by PerkinElmer Victor Light 1420 Luminescence Counter (PerkinElmer, Waltham, Massachusetts) according to the manufacturer's guidelines. Concentration that inhibits 50% (IC$_{50}$) values and graphs were determined by

Sigmaplot 12.0 software (Systat Software Inc., San Jose, California) and GraphPad Prism 6 software (GraphPad Software, San Diego, California). These experiments were repeated three times independently.

Immunoblot Assay and Phospho-Receptor Tyrosine Kinase Array

Cells were plated on 6-well plates and treated with 100 nM and 1 μM EGFR TKIs for 4 hours. Subsequently, cells were lysed with 10X cell lysis buffer (Cell Signaling Technology, Danvers, Massachusetts), phenyl-methylsulfonyl fluoride (Sigma, St. Louis, Missouri), PhosSTOP (Roche, Basel, Switzerland), and proteinase inhibitor cocktail (Merck, Kenilworth, New Jersey). Cell lysates were quantified with protein assay dye reagent concentrate (Bio-Rad, Hercules, California). Prepared samples were separated through NuPAGE Bis-Tris Gels (Invitrogen) and transferred to polyvinylidene difluoride membranes (Bio-Rad). Protein bands were visualized with ECL Prime Western Blotting Detection Reagent (GE Healthcare, Chicago, Illinois). Total EGFR (#4267s), phospho-EGFR (#3777s), total signal transducer and activator of transcription 3 (STAT3) (#4904), phospho-STAT3 (#9134), total AKT (#4685), phospho-AKT (#4060s), total ERK p42/p44 (#9102), phospho-ERK (#9106), and glyceraldehyde-3-phosphate dehydrogenase (GAPDH) (#5174) antibodies were used to analyze the EGFR signaling pathway; antibodies were purchased from Cell Signaling Technology. Imaging analysis was performed with ImageQuant LAS4000mini (GE Healthcare) according to the manufacturer's guidelines.

SNU-3173 Colony-Forming Assay

SNU-3173 cells were plated at 1×10^3/well in 12-well plates with RPMI-1640 media and incubated overnight. After cells adhered, osimertinib was added at 50, 100, and 500 nM. Drugs and media were changed every 3 days for 3 weeks. Cells were washed twice with Dulbecco's Phosphate-Buffered Saline (Gibco), fixed for 30 minutes in absolute ethanol at room temperature, and washed with distilled water. Cells were stained for 10 minutes with 0.1% Brilliant Blue (Sigma-Aldrich) and washed three times with distilled water. Stained cells were captured and counted with the EVOS Cell Imaging System (Thermo Fisher, Waltham, Massachusetts).

Polymerase Chain Reaction and Quantitative Real-Time Polymerase Chain Reaction

Genomic DNA was isolated from the SNU-3173 patient-derived cell line and Ba/F3 cells containing *EGFR* exon 20 insertion mutations, including *EGFR* A763insFQEA, V769insASV, D770insSVD, P772insPR, H773insH, and H773insNPH using an ALL-prep DNA/

RNA micro kit (Qiagen, Venlo, Netherlands). *EGFR* exons were amplified with specifically designed primers (Supplementary Table 1) using the High Fidelity Plus polymerase chain reaction (PCR) System (Roche). Cycling conditions were 95°C for 10 minutes, followed by 35 cycles at 95°C for 20 seconds, 58°C for 30 seconds, and 72°C for 30 seconds. Exons were sequenced by the Sanger sequencing method using specific primers.

Computational Atomistic Modeling of EGFR Exon 20 Insertion and Docking Simulation

EGFR wild-type (PDB ID: 4ZAU), L858R/T790M (PDB ID: 4RJ5), and D770_N771insNPG (PDB ID: 4LRM) protein crystallization models were developed using the Protein Data Bank (http://www.rcsb.org/pdb/). Predictive models of other EGFR exon 20 insertion–mutant proteins (A763insFQEA, V769insASV, D770insSVD, P772insPR, H773insH, H773insNPH, and H773insAH) were constructed.[11] Docking simulations of these atomistic models with osimertinib were processed.[12] Constructed models and docking simulations were visualized and analyzed using the University of California San Francisco (UCSF) Chimera software.[13]

ENU Mutagenesis Screening and Osimertinib-Resistant (SNU-3173OR) Model

EGFR exon 20 insertion–mutant Ba/F3 cells were plated at 5×10^6 cells/mL and exposed to 50 μg/mL ENU for 24 hours. After exposure to ENU, Ba/F3 cells harboring *EGFR* exon 20 insertion mutations were washed with RPMI-1640 three times and cultured for exponential growth. ENU-exposed cells were plated on 96-well plates with 1 μM osimertinib in RPMI-1640 media. Cells were inspected by light microscopy at 2- to 4-day intervals and media with compounds were changed. *EGFR* exons 18 to 25 were amplified from DNA extracts of cells by polymerase chain reaction and analyzed by directed sequencing.

SNU-3173OR cell lines were developed through osimertinib dose escalation. Osimertinib concentrations were increased in a stepwise manner from 50 nM to 1 μM depending on cell confluence. After osimertinib resistance, defined as cell growth at 1 μM of osimertinib developed, cells were maintained on 500 nM osimertinib.

Results
Construction and Characterization of EGFR Exon 20 Insertion Models

Common subtypes of *EGFR* exon 20 insertion mutations were selected based on the Catalogue of Somatic Mutations in Cancer (COSMIC) database to evaluate EGFR TKI efficacy against numerous *EGFR* exon 20 insertion subtypes using Ba/F3 and a patient-derived

cell line model.[14] Seven *EGFR* exon 20 insertion muta-tions with variable *EGFR* mRNA expression, which represents approximately 60% of mutations, were selected: *EGFR* A763insFQEA (5.1%), V769insASV (21.9%), D770insSVD (14.8%), D770insNPG (not appli-cable), P772insPR (5.6%), H773insNPH (8.7%), and H773insH (3.6%) (Fig. 1*A*, Supplementary Fig. 1, and Supplementary Table 2). All *EGFR* exon 20 insertion

mutant Ba/F3 cells spontaneously grew without IL-3, suggesting oncogenic potential (Fig. 1*B*).

Cell Proliferation and Immunoblot Assays

Cell viability assay was performed to estimate sensitivity to EGFR TKIs in *EGFR* exon 20 insertion–mutant cell lines. All constructed *EGFR* exon 20
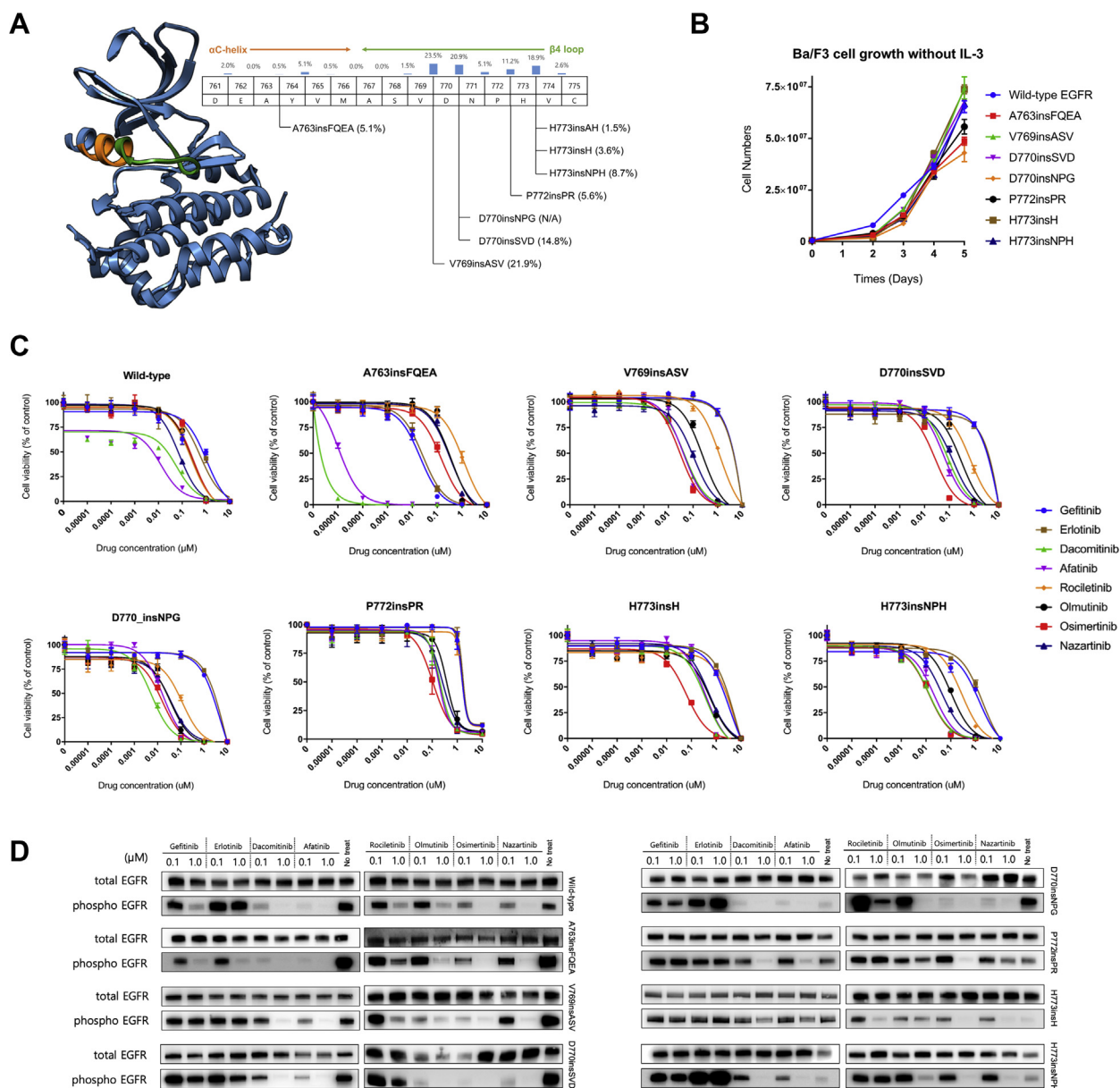

Figure 1. *EGFR* exon 20 insertion mutations and their in vitro characteristics. (*A*) Crystal structure of EGFR (PDB ID: 4ZAU) and frequency of *EGFR* exon 20 insertion mutations. Color-marked ribbon diagram shows *EGFR* exon 20 insertion regions of C-helix and loop following C-helix colored with *orange* and *green*, respectively. (*B*) *EGFR* exon 20 insertion mutant Ba/F3 cells were selected and cultured in the absence of interleukin-3 (IL-3). All cells grew exponentially without IL-3 due to their oncogenic potential. *EGFR* wild-type cells were cultured with 30 ng/mL epidermal growth factor (EGF)–containing media. (*C*) Cell viability assays of Ba/F3 cells harboring *EGFR* exon 20 insertion mutations using EGFR tyrosine kinase inhibitors (TKIs). All cells were exposed to EGFR TKIs for 72 hours. These experiments were repeated three times independently, and graphs represent mean values. (*D*) Immunoblot assays of *EGFR* exon 20 insertion–mutant Ba/F3 cells. Cells were exposed to EGFR TKIs for 4 hours to detect inhibition of EGFR phosphorylation and other signaling pathways.

Table 1. IC$_{50}$ Values of EGFR-Mutant Cells

IC$_{50}$ (nM) Mean / S.D.	WT (+EGF) 30 ng/mL	FQEA	ASV	SVD	NPG	PR	H	NPH	SNU-3173	PC9	H1975	A549
Gefitinib	1127 / 90	21.7 / 4	4870.1 / 288.5	3479.3 / 790.9	2422 / 267.3	3611.4 / 1178.1	1980.1 / 288.7	948.7 / 138.5	1050.4 / 66.8	10.9	7212.2	3716
Erlotinib	1333.1 / 173.3	33.3 / 5.1	5050.7 / 520.5	5179.7 / 393.3	3240.1 / 289.7	5391 / 115.1	2858.7 / 337.2	1391 / 236.6	4535.5 / 321	14.9	5409.3	2950.2
Dacomitinib	39 / 4.4	0.002 / 0.00019	55.4 / 2.1	85.9 / 3.8	7.5 / 0.7	161.8 / 18.7	320.2 / 34.8	10.8 / 1.8	13.7 / 1.6	0.0043	83.5	1482.3
Afatinib	7.3 / 0.4	0.013 / 0.00092	54.1 / 3.3	63.8 / 6.7	16.7 / 2.1	200 / 10.4	352.5 / 22.7	19.5 / 3	16.7 / 2.2	0.0232	96	1158.4
Rociletinib	262.9 / 25.7	1022.1 / 172.8	1324.9 / 66.7	731.8 / 61.1	96.7 / 12.9	3034.6 / 689.8	2309.4 / 401.4	288 / 25	1202.5 / 158.2	62.8	24.2	3123
Olmutinib	236.2 / 16.4	351.8 / 20.2	262.3 / 20.8	287.7 / 29.5	30.4 / 3.9	314.3 / 27.6	497.6 / 50.5	97.3 / 2.7	626.7 / 31.6	8.5	3.3	5062.3
Osimertinib	259.2 / 22.7	131.6 / 19	41 / 4.0	28.1 / 2.9	14.7 / 2.2	22.4 / 3.9	65.7 / 4.5	11.4 / 1.3	62.7 / 7.3	0.52	1.5	1609.9
Nazartinib	82.4 / 4.9	351.8 / 28.6	108.2 / 6.9	128.5 / 17	36.3 / 4.1	147.7 / 13.4	509.9 / 58.4	49.6 / 1.8	139.7 / 13.6	4.2	12.8	2782

IC$_{50}$ values were calculated from cell viability assays. Human lung cancer cell lines, PC9 (exon 19 in-frame deletion, E746-A750del), NCI-H1975 (EGFR L858R/T790M), and A549 (KRAS G12S) were used as controls for EGFR TKIs.

EGF, epidermal growth factor; IC$_{50}$, concentration that inhibits 50%; WT, wild-type; TKI, tyrosine kinase inhibitor; FQEA, A763insFQEA; ASV, V769insASV; SVD, D770insSVD; NPG, D770insNPG; PR, P772insPR; H, H773insH; NPH, H773insNPH.

insertion–mutant Ba/F3 cells, except *EGFR* A763insFQEA, were resistant to first-generation EGFR TKIs (IC$_{50}$ > 3.3 ± 0.4μM) (Table 1). Although *EGFR* A763insFQEA, D770insNPG, and H773insNPH mutants were highly sensitive to afatinib and dacomitinib, other *EGFR* exon 20 insertion mutants were resistant to these agents. Among the third-generation EGFR TKIs, osimertinib was highly active against *EGFR* exon 20 insertion–mutant Ba/F3 cells (IC$_{50}$, 11.4 ± 1.3 to 65.7 ± 4.5nM), except for *EGFR* A763insFQEA (IC$_{50}$, 131.6 ± 19nM) (Table 1 and Supplementary Fig. 2). In addition, the *EGFR* H773insH–mutant model, which showed the highest oncogenic potential and resistance to most EGFR TKIs, was moderately sensitive to osimertinib (Fig. 1*C*).

Next, immunoblot assays were performed to validate the results of cell viability assays. The expression of phospho-EGFR was downregulated by the EGFR TKIs that were found to elicit dose-dependent sensitivity in cell viability assays. Similarly, osimertinib downregulated expression of phospho-EGFR in all *EGFR* exon 20 insertion models, including *EGFR* H773insH (Fig. 1*D* and Supplementary Fig. 3).

Cell Viability and Immunoblot Assays in SNU-3173

The SNU-3173 cell line was established from malignant pleural effusions of a chemo-naive, 46-year-old man diagnosed with stage IV lung adenocarcinoma and an *EGFR* H773insAH mutation in exon 20 confirmed by direct sequencing (Fig. 2*A*). Osimertinib showed the third highest potency against SNU-3173 cells (Fig. 2*B*) and remarkable inhibition of phospho-EGFR and phospho-ERK signals (Fig. 2*C*). In addition, colony-forming assays were performed to functionally investigate the inhibitory capacity of osimertinib in SNU-3173 cells. Osimertinib at 50 nM significantly inhibited the growth of SNU-3173 cells (Fig. 2*D*). Regarding the IC$_{50}$ ratio in *EGFR* mutant versus wild-type cells, osimertinib showed lowest IC$_{50}$ values in *EGFR* exon 20 insertion–mutant Ba/F3 cells, except *EGFR* A763insFQEA, and in SNU-3173 cells, suggesting milder predictive toxicity compared with that of other EGFR TKIs (Fig. 3).

Homology Models of EGFR Exon 20 Insertion Mutations

Because insertion sites and inserted amino acids vary, EGFR TKIs showed different efficacies against *EGFR* exon 20 insertion mutations. Therefore, we developed homology models of selected *EGFR* exon 20 insertion mutants and compared EGFR crystal structures to estimate how insertion mutants changed
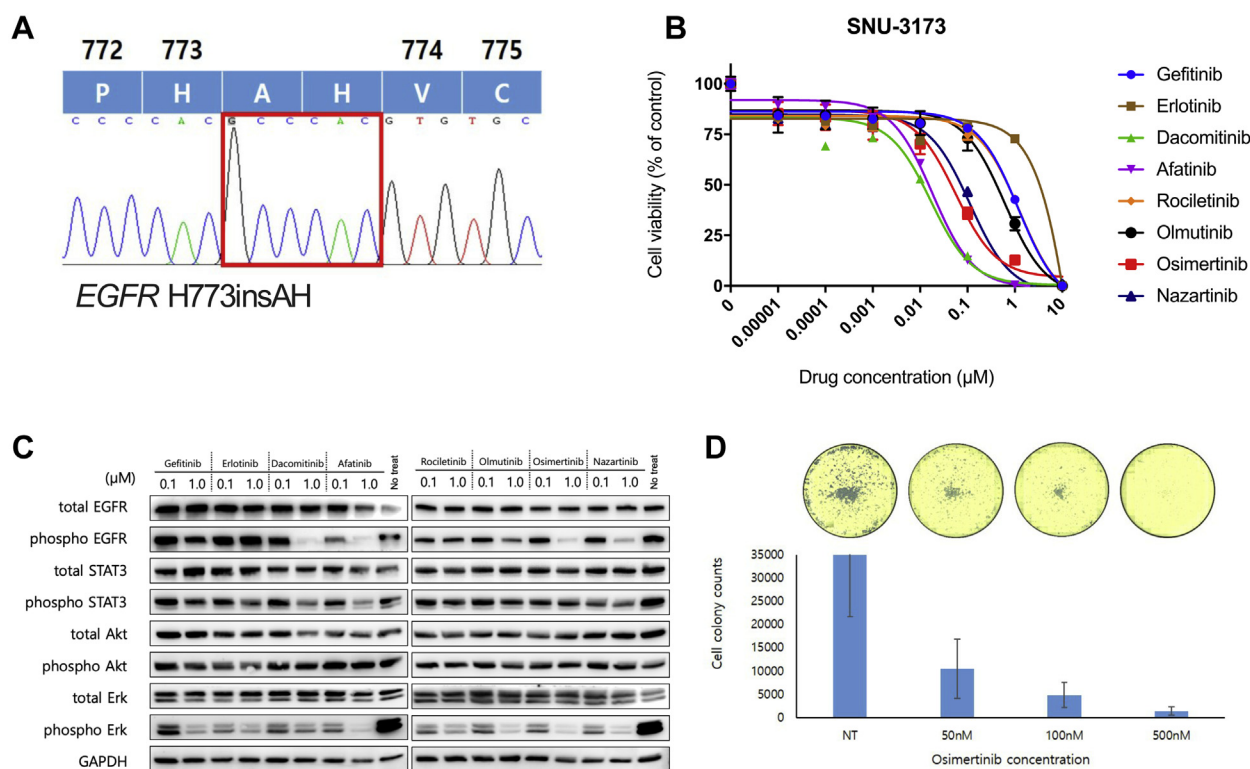
Figure 2. Characterization of patient-derived SNU-3173 cells with *EGFR* exon 20 insertion mutation. (*A*) Direct sequencing of patient-derived SNU-3173 cell line with *EGFR* H773insAH mutation. (*B*) Cell viability assay of SNU-3173 cells with various EGFR TKIs. (*C*) Immunoblot assay of SNU-3173 cell line. Cells were exposed to 100 nM and 1 μM EGFR TKI for 4 hours to detect EGFR phosphorylation and other signaling pathways. (*D*) Colony-forming assay of SNU-3173 cells. Cells were seeded and exposed to osimertinib for 3 weeks. These experiments were repeated three times independently, and graphs represent mean values.

EGFR structures (Supplementary Fig. 4). We merged EGFR L858R/T790M (PDB ID: 4RJ5) and EGFR D770insNPG (PDB ID: 4LRM) to discover structural differences (Fig. 4*A*). The inserted amino acids pushed the

Figure 3. *EGFR* mutant to wild-type IC$_{50}$ ratios of EGFR TKIs against *EGFR*-mutant cells. *EGFR* mutant to wild-type IC$_{50}$ ratios were calculated as concentration that inhibits 50% (IC$_{50}$) values of *EGFR*-mutant cells divided by those of *EGFR* wild-type cells. The smaller value predicts smaller toxicities associated with sparing of wild-type EGFR cells. Individual values were calculated from Table 1. PC9, H1975, and A549 cells were used as controls for EGFR TKIs.

C-helix and the following loop bidirectionally, resulting in structural distortion. Because of the insertions, the P-loop bent into the drug-binding site and impeded drug entry. In addition, the twisted structure pushed out the activation loop, such that the distorted structure favored adenosine triphosphate (ATP) binding, stable dimerization, and signaling protein activation. In addition, a coupling model between osimertinib and EGFR exon 20 insertions was simulated to discover how osimertinib could bind EGFR exon 20 insertion mutations. Although the push-down effect of the P-loop allows the binding pocket to narrow and hinder EGFR TKI binding, osimertinib can flexibly enter the drug-binding pocket (Fig. 4*B*). In addition, we compared IC$_{50}$ values and docked osimertinib on EGFR H773insAH and wild-type EGFR (Supplementary Fig. 5). Consistent with IC$_{50}$ values (62.7 nM and 259.2 nM, respectively), osimertinib showed flexible access to the drug-binding pocket of EGFR H773insAH (Supplementary Fig. 6).
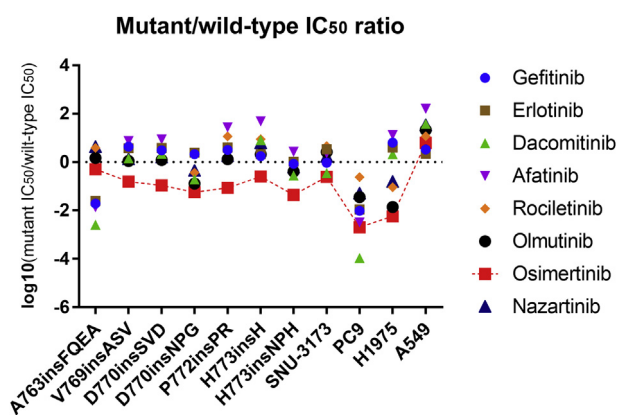
EGFR Mutational Spectrum of Osimertinib Resistance

Although osimertinib potently inhibits *EGFR* exon 20 insertions, acquired resistance is inevitable. Thus, we
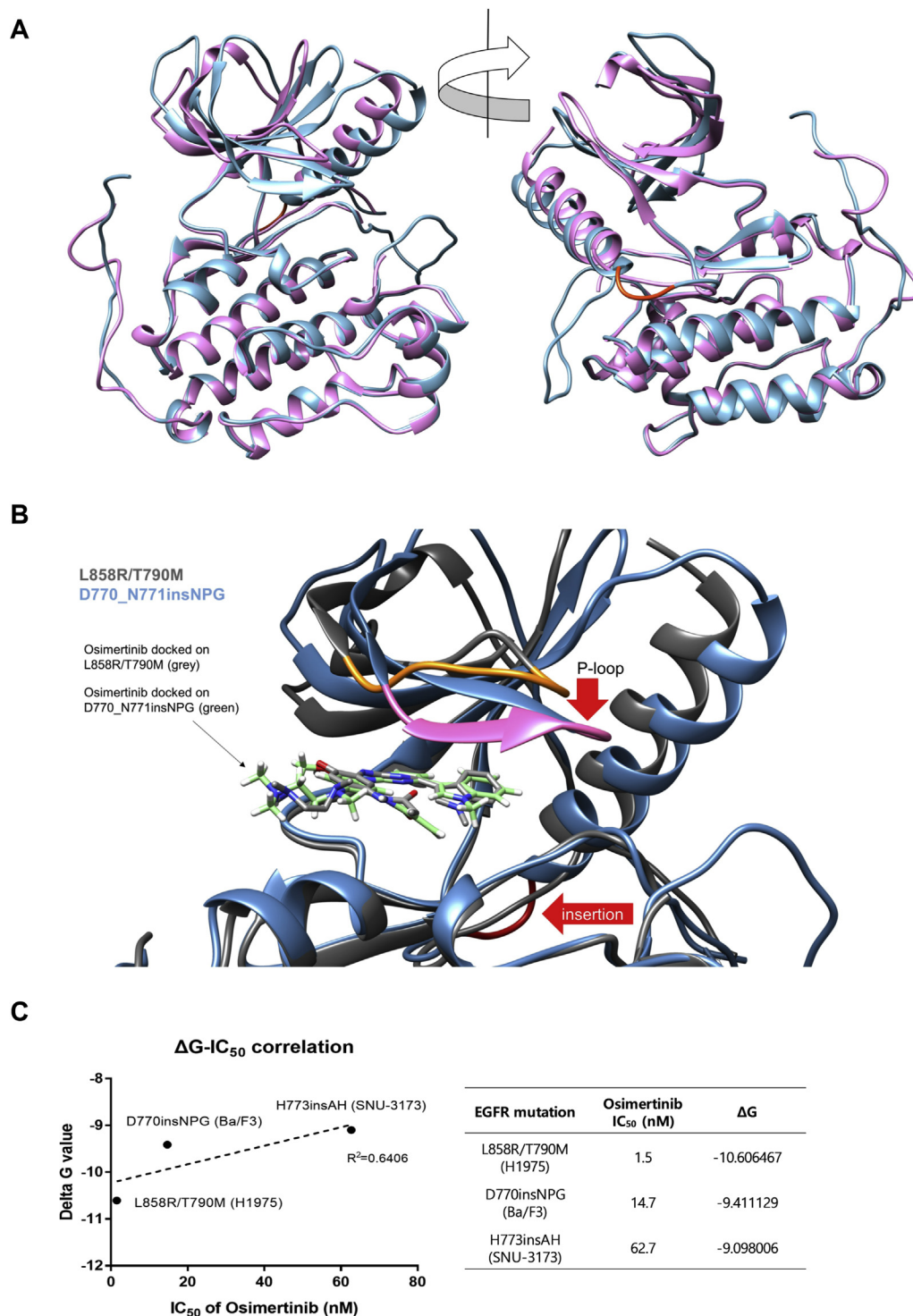
Figure 4. Docking simulation of osimertinib on merged crystal structures of mutant EGFR proteins. (*A*) EGFR L858R/T790M (PDB ID: 4RJ5, *pink*) and D770insNPG (PDB ID: 4LRM, *light blue*) were merged. Structures were turned and showed both the drug-binding side and the Asparagine-Proline-Glycine (NPG) amino acids-inserted side. (*B*) Previously constructed crystal structures of the EGFR mutants with *grey*- and partial *orange*-colored ribbons and *blue*- and partial *pink*-colored ribbons indicate EGFR L858R/T790M mutation (PDB ID: 4RJ5) and D770insNPG mutation (PDB ID: 4LRM), respectively. Osimertinib docked on EGFR L858R/T790M and D770insNPG are indicated as *grey* and *green*, respectively. *Red arrows* indicate structural changes between models. (*C*) Correlation of IC_{50} values and docking simulation for EGFR L858R/T790M, D770inNPG, and H773insAH. Structures were handled with UCSF Chimera.
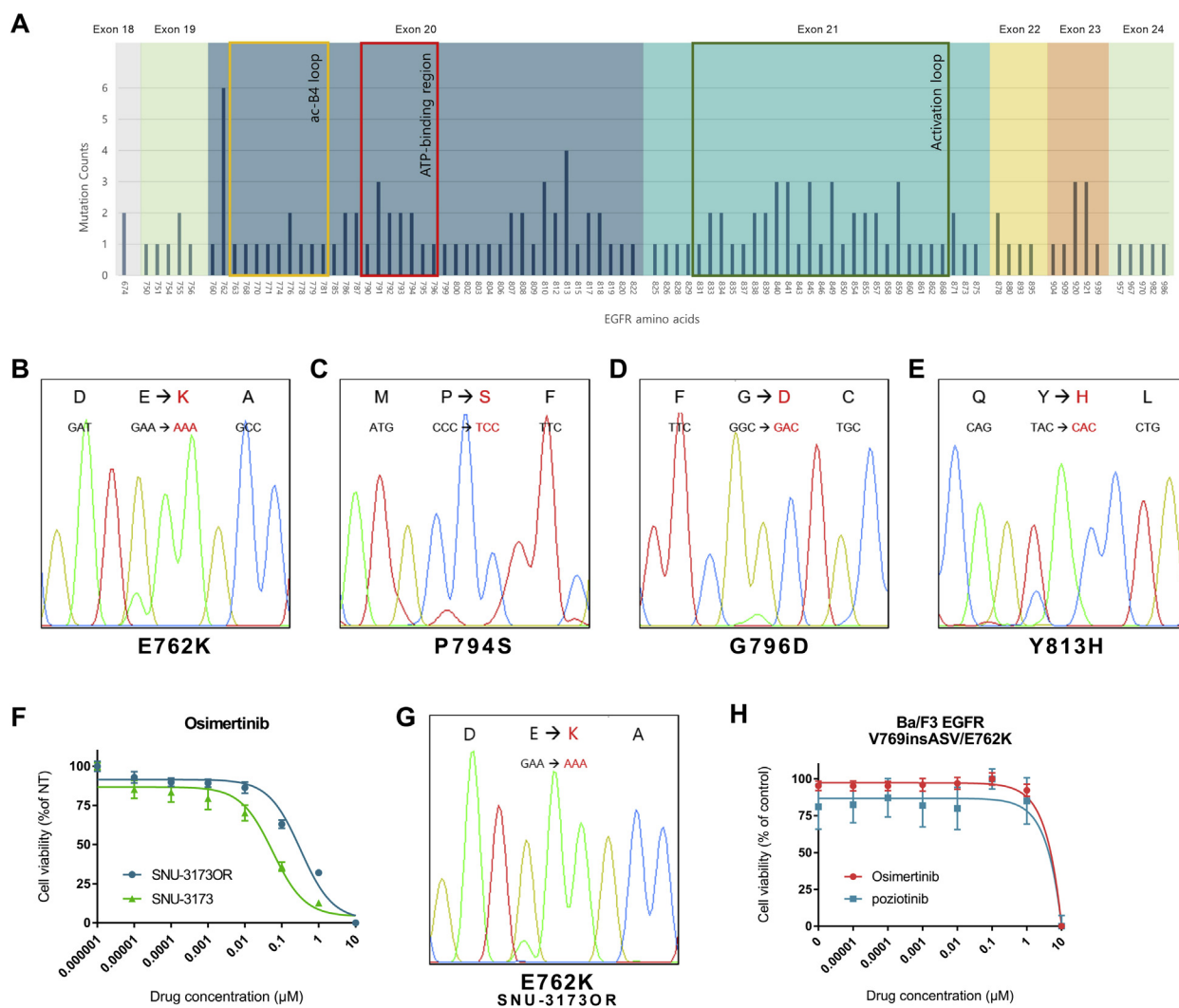
Figure 5. Osimertinib resistance screening through ENU mutagenesis and development of osimertinib resistant SNU-3173 cells. (*A*) Screened *EGFR* mutations from ENU mutagenesis screening. (*B-E*) Direct sequencing results of hotspot *EGFR* mutations associated with acquired resistance to osimertinib. (*F*) Cell viability assays of osimertinib-resistant SNU-3173 (SNU-3173OR) and SNU-3173 cells (*G*). SNU-3173OR cells showed *EGFR* E762K mutation. (*H*) Cell viability assay of EGFR V769insASV/E762K–mutant Ba/F3 cells. Cells were treated with osimertinib and poziotinib for 72 hours. Graph represents mean ± SD, and the experiments were repeated three times.

performed ENU mutagenesis screening to identify additional *EGFR* mutations related to osimertinib resistance. Ba/F3 cells harboring *EGFR* D770insSVD, H773insH, and H773insNPH were exposed to ENU and selected during exposure to osimertinib (Fig. 5*A*). The most frequent mutations occurred at *EGFR* E762, which is before the region of the insertion mutations. In addition, numerous and diverse mutations were located in the ATP-binding pocket in exon 20 and activation loop in exon 21 (Supplementary Table 3). *EGFR* L792I/S, P794S, and G796D mutations were identified as mechanisms of resistance to third-generation EGFR TKIs in previous studies (Figs. 5*C* and *D*).[15-21] Those located near the ATP-binding region could hinder osimertinib binding. However, although *EGFR* C797S conferred resistance to

osimertinib in *EGFR* exon 20 insertion mutant cells (Supplementary Fig. 7), that was not identified through our ENU mutagenesis screening. Simultaneously, we developed an osimertinib-resistant cell line, SNU-3173OR (Fig. 5*F*). *EGFR* E762K, which was the most frequent mutation identified by ENU mutagenesis screening, was also identified in these cells (Fig. 5*G*). *EGFR* V769insASV/E762K-mutant Ba/F3 and 293T cells conferred resistance to osimertinib as well as poziotinib (Fig. 5*H* and Supplementary Fig. 8).

Discussion

Our study has shown that osimertinib is active against *EGFR* exon 20 insertion-mutant models and patient-derived SNU-3173 cells. In addition, the *EGFR*

exon 20 insertion mutant to wild-type ratios of half-maximal inhibitory concentrations were significantly lower for osimertinib than for other EGFR TKIs. Homology models revealed that osimertinib binds the drug-binding pocket of EGFR D770insNPG, similar to EGFR L858R/T790M. Regarding mechanisms of osimertinib resistance, *EGFR* E762K was the most common mutation identified through ENU mutagenesis screening of Ba/F3 cells and was also found in osimertinib-resistant SNU-3173 cells.

Osimertinib is highly active in *EGFR* exon 20 insertion models, except *EGFR* A763insFQEA, which is sensitive to first-generation EGFR TKIs.[22] Furthermore, Ba/F3 cells harboring *EGFR* H773insH, which was resistant to most EGFR TKIs, showed toxicity in response to osimertinib. Although osimertinib had limited in vitro or in vivo efficacy in *EGFR* exon 20 insertion models, three models (*EGFR* H773HVdup, H773insNPH, and P772insDNP) did not represent heterogeneous *EGFR* exon 20 insertion mutations.[23,24] Recently, osimertinib showed antitumor activity in NCI-H2073 cells with *EGFR* D770insSVD and V769insASV and in three activating αC-β4 loop-insertion mutations (*EGFR* D770insG, D770>GY, and N771insN) consistent with our results.[25,26]

In our study, we developed seven EGFR exon 20 insertion models and one patient-derived cell line, comprising approximately 60% of all *EGFR* exon 20 insertion mutations based on the COSMIC database.[14] Our EGFR TKI screening of eight mutant models is the largest study of EGFR exon 20 insertions, showing superior anticancer activity of osimertinib. Although poziotinib was identified as a potent inhibitor for *EGFR* exon 20 insertion mutations through in silico, in vitro, and in vivo tests in line with our in vitro data (Supplementary Fig. 9), 55% to 60% of patients require dose reduction due to adverse events related to wild-type EGFR inhibition.[8] In addition, despite a high ORR (55%), median PFS was only 5.5 months, suggesting that an alternative treatment option is necessary for NSCLC patients with *EGFR* exon 20 insertion mutations such as afatinib or osimertinib plus cetuximab combination strategy.[7,27] Considering the low mutant to wild-type ratio of IC$_{50}$ that might be a biased parameter, osimertinib might be an alternative treatment for patients with NSCLC and EGFR exon 20 insertions as in a promising NSCLC case of *EGFR* D770insSVD mutation that responded to osimertinib.[28]

Structurally, we constructed homology models of EGFR exon 20 insertions. If EGFR exon 20 insertions make a wrinkle or a wide curve that pushes the C-helix and loop bilaterally, these structural changes permit the entrance of the drug-binding pocket to narrow and block drug activity. This steric hindrance was mediated by shifts of the P-loop and the αC-helix into the drug-binding pockets in three-dimensional modeling of EGFR D770insNPG. In this model, the narrow drug-binding pocket sterically hindered osimertinib binding.[8,9] However, our simulation model revealed that osimertinib binds to the drug-binding pockets of EGFR D770insNPG and EGFR L858R/T790M in similar manners.

The identification of mechanisms of acquired resistance to osimertinib is important to guide subsequent treatment. Therefore, we screened osimertinib-resistant *EGFR* mutations using an ENU mutagenesis method. *EGFR* mutations at sites E762 and Y813 were commonly found in screened cells. EGFR E762 was conserved at the αC-helix in the N lobe of the EGFR kinase and formed a K745-E762 salt bridge, which mediates the "αC-in" or "αC-out" conformation.[29] Although *EGFR* E762K was identified as the mutation most likely to bind gefitinib, this was observed only in sporadic breast cancer and not in NSCLC.[15,30] In our functional analysis, *EGFR* E762K mutation conferred resistance to osimertinib as well as poziotinib. In addition, *EGFR* P794S and G796D mutations near the C797 site were observed in our mutagenesis screening studies and are known as osimertinib resistance mechanisms.[15,16] Diverse and numerous sites of *EGFR* mutations might limit the long-term efficacy of osimertinib in NSCLC with *EGFR* exon 20 insertion mutations. However, it is cautious to evaluate osimertinib resistance mechanisms using Ba/F3 and ENU mutagenesis models only due to diverse non-EGFR–mediated resistance mechanisms.

In conclusion, osimertinib showed potent growth inhibition of most *EGFR* exon 20 insertion mutant cells with superior sparing of wild-type *EGFR* cells. Furthermore, osimertinib binds in the drug-binding pocket of insertion mutant EGFR exon 20. Various osimertinib-resistant *EGFR* mutations, including *EGFR* E762K, were identified by ENU mutagenesis screening of *EGFR* exon 20 insertion-mutant cells. Our results have led to the initiation of a phase II trial of osimertinib at 80 mg once daily (NCT03414814) in Korean patients with NSCLC and *EGFR* exon 20 insertion mutations. In addition, these data support the ongoing phase II trial of osimertinib at 160 mg once daily (NCT03191149) in western NSCLC patients with *EGFR* exon 20 insertion mutations. Although the ORR of osimertinib to EGFR exon 20 insertion–positive NSCLC was only 6% in a retrospective study, clinical outcomes of prospective trials might lead to a mutation subtype-specific approach for treating NSCLC patients with *EGFR* exon 20 insertion mutation similar to our variable in vitro efficacies of osimertinib.[31]

Acknowledgments

Supplementary Data

Note: To access the supplementary material accompanying this article, visit the online version of the *Journal of Thoracic Oncology* at www.jto.org and at https://doi.org/10.1016/j.jtho.2019.05.006.

References

1. Shin A, Oh CM, Kim BW, et al. Lung cancer epidemiology in Korea. *Cancer Res Treat*. 2017;49:616-626.
2. Siegel RL, Miller KD, Jemal A. Cancer statistics, 2018. *CA Cancer J Clin*. 2018;68:7-30.
3. Herbst RS, Morgensztern D, Boshoff C. The biology and management of non-small cell lung cancer. *Nature*. 2018;553:446-454.
4. Seo JS, Ju YS, Lee WC, et al. The transcriptional landscape and mutational profile of lung adenocarcinoma. *Genome Res*. 2012;22:2109-2119.
5. Chong CR, Janne PA. The quest to overcome resistance to EGFR-targeted therapies in cancer. *Nat Med*. 2013;19:1389-1400.
6. Yasuda H, Kobayashi S, Costa DB. EGFR exon 20 insertion mutations in non-small-cell lung cancer: preclinical data and clinical implications. *Lancet Oncol*. 2012;13:e23-e31.
7. Yang JC, Wu YL, Schuler M, et al. Afatinib versus cisplatin-based chemotherapy for EGFR mutation-positive lung adenocarcinoma (LUX-Lung 3 and LUX-Lung 6): analysis of overall survival data from two randomised, phase 3 trials. *Lancet Oncol*. 2015;16:141-151.
8. Robichaux JP, Elamin YY, Tan Z, et al. Mechanisms and clinical activity of an EGFR and HER2 exon 20-selective kinase inhibitor in non-small cell lung cancer. *Nat Med*. 2018;24:638-646.
9. Heymach J, Negrao M, Robichaux J, et al. OA02.06 A phase II trial of poziotinib in EGFR and HER2 exon 20 mutant non-small cell lung cancer (NSCLC). *J Thorac Oncol*. 2018;13:S323-S324.
10. Greulich H, Chen TH, Feng W, et al. Oncogenic transformation by inhibitor-sensitive and -resistant EGFR mutants. *PLoS Med*. 2005;2:e313.
11. Waterhouse A, Bertoni M, Bienert S, et al. SWISS-MODEL: homology modelling of protein structures and complexes. *Nucleic Acids Res*. 2018;46:W296-W303.
12. Grosdidier A, Zoete V, Michielin O. SwissDock, a protein-small molecule docking web service based on EADock DSS. *Nucleic Acids Res*. 2011;39:W270-W277.
13. Pettersen EF, Goddard TD, Huang CC, et al. UCSF Chimera—a visualization system for exploratory research and analysis. *J Comput Chem*. 2004;25:1605-1612.
14. Sondka Z, Bamford S, Cole CG, et al. The COSMIC Cancer Gene Census: describing genetic dysfunction across all human cancers. *Nat Rev Cancer*. 2018;18:696-705.
15. Martinez-Jimenez F, Overington JP, Al-Lazikani B, et al. Rational design of non-resistant targeted cancer therapies. *Sci Rep*. 2017;7:46632.
16. Klempner SJ, Mehta P, Schrock AB, et al. Cis-oriented solvent-front EGFR G796S mutation in tissue and ctDNA in a patient progressing on osimertinib: a case report and review of the literature. *Lung Cancer (Auckl)*. 2017;8:241-247.
17. Zheng D, Hu M, Bai Y, et al. EGFR G796D mutation mediates resistance to osimertinib. *Oncotarget*. 2017;8:49671-49679.
18. Thress KS, Paweletz CP, Felip E, et al. Acquired EGFR C797S mutation mediates resistance to AZD9291 in non-small cell lung cancer harboring EGFR T790M. *Nat Med*. 2015;21:560-562.
19. Le X, Puri S, Negrao MV, et al. Landscape of EGFR-dependent and -independent resistance mechanisms to osimertinib and continuation therapy beyond progression in EGFR-mutant NSCLC. *Clin Cancer Res*. 2018;24:6195-6203.
20. Yang Z, Yang N, Ou Q, et al. Investigating novel resistance mechanisms to third-generation EGFR tyrosine kinase inhibitor osimertinib in non-small cell lung cancer patients. *Clin Cancer Res*. 2018;24:3097-3107.
21. Ou SI, Cui J, Schrock AB, et al. Emergence of novel and dominant acquired EGFR solvent-front mutations at Gly796 (G796S/R) together with C797S/R and L792F/H mutations in one EGFR (L858R/T790M) NSCLC patient who progressed on osimertinib. *Lung Cancer*. 2017;108:228-231.
22. Yasuda H, Park E, Yun CH, et al. Structural, biochemical, and clinical characterization of epidermal growth factor receptor (EGFR) exon 20 insertion mutations in lung cancer. *Sci Transl Med*. 2013;5:216ra177.
23. Cross DA, Ashton SE, Ghiorghiu S, et al. AZD9291, an irreversible EGFR TKI, overcomes T790M-mediated resistance to EGFR inhibitors in lung cancer. *Cancer Discov*. 2014;4:1046-1061.
24. Yang M, Xu X, Cai J, et al. NSCLC harboring EGFR exon-20 insertions after the regulatory C-helix of kinase domain responds poorly to known EGFR inhibitors. *Int J Cancer*. 2016;139:171-176.
25. Floc'h N, Martin MJ, Riess JW, et al. Antitumor activity of osimertinib, an irreversible mutant-selective EGFR tyrosine kinase inhibitor, in NSCLC harboring EGFR exon 20 insertions. *Mol Cancer Ther*. 2018;17:885-896.
26. Ruan Z, Kannan N. Altered conformational landscape and dimerization dependency underpins the activation of EGFR by alphaC-beta4 loop insertion mutations. *Proc Natl Acad Sci U S A*. 2018;115:E8162-E8171.
27. Hasegawa H, Yasuda H, Hamamoto J, et al. Efficacy of afatinib or osimertinib plus cetuximab combination

therapy for non-small-cell lung cancer with EGFR exon 20 insertion mutations. *Lung Cancer*. 2019;127:146–152.

28. Piotrowska Z, Fintelmann FJ, Sequist LV, et al. Response to osimertinib in an EGFR exon 20 insertion-positive lung adenocarcinoma. *J Thorac Oncol*. 2018;13:e204-e206.

29. Shan Y, Eastwood MP, Zhang X, et al. Oncogenic mutations counteract intrinsic disorder in the EGFR kinase and promote receptor dimerization. *Cell*. 2012;149:860–870.

30. Weber F, Fukino K, Sawada T, et al. Variability in organ-specific EGFR mutational spectra in tumour epithelium and stroma may be the biological basis for differential responses to tyrosine kinase inhibitors. *Br J Cancer*. 2005;92:1922–1926.

31. van Veggel B, De Langen J, van der Wekken A, et al. 1450POsimertinib treatment for patients with EGFR exon 20 insertion positive non-small cell lung cancer. *Ann Oncol*. 2018;29.